Journal of Materials Chemistry C

PAPER

View Article Online
View Journal | View Issue

CrossMark click for updates

Cite this: J. Mater. Chem. C, 2016, 4, 11474

FTC-containing molecules: large second-order nonlinear optical performance and excellent thermal stability, and the key development of the "Isolation Chromophore" concept†

Pengyu Chen,[a] Xiuyang Yin,[a] Yujun Xie,[a] Shufang Li,[b] Shiyu Luo,[a] Huiyi Zeng,[b] Guocong Guo,[b] Qianqian Li[a] and Zhen Li*[a]

Received 2nd October 2016,
Accepted 7th November 2016

DOI: 10.1039/c6tc04282a

www.rsc.org/MaterialsC

A series of second-order nonlinear optical (NLO) molecules, **M1–M5**, were designed and successfully synthesized through the convenient "click chemistry" reaction, which contain two different types of chromophore moieties, the FTC chromophore and nitro-based azo ones, according to the concept of "Isolation Chromophore". All these five molecules possess excellent thermal stability and very large NLO performance, with an ultrahigh d_{33} value of 384 pm V^{-1} at the wavelength of 1950 nm achieved for **M1**, furthering the rational design of excellent NLO materials.

Introduction

In the past few decades, considerable interest has been paid to organic second-order nonlinear optical (NLO) materials, due to their huge potential applications in a variety of fields such as ultrafast optical switches, high-speed optical modulators, high-density optical data storage and so on.[1] Compared to conventional inorganic crystalline materials, organic second-order nonlinear optical (NLO) materials have numerous advantages, including good processability, ultrafast response time and superior chemical flexibility. In the organic NLO field, how to translate the large microscopic β values of the organic chromophores into high macroscopic NLO activities of the NLO polymers effectively is the major problem and challenge.[2] Generally, because of the strong dipole–dipole interactions between the chromophore moieties with a donor–π–acceptor (D–π–A) structure, the chromophore moieties could not be efficiently and absolutely poled to the required noncentrosymmetric alignment for the realization of the macroscopic NLO effect, during the poling process under an electric field (Fig. 1A), but easy to be relaxed upon the removal of the electric field or the increase of temperature.[3]

With the appropriate design of molecular structures, the dipole–dipole interactions between the chromophore moieties could be weakened to a large degree.[4] A lot of work has been conducted about this stuff by many researchers. Based on their excellent work, we have done systematic research studies on NLO polymers, including linear polymers, dendronized polymers, dendrimers (including the recently developed Janus NLO

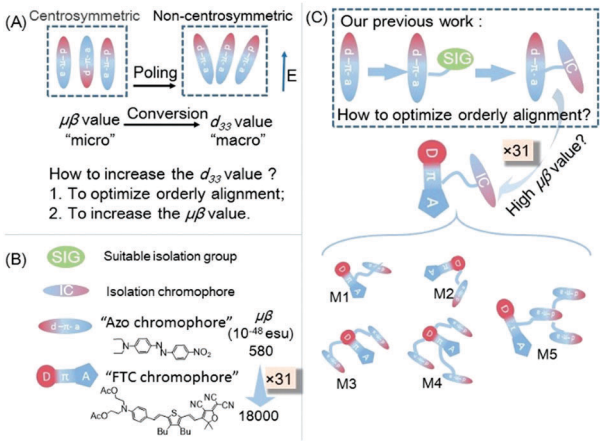

Fig. 1 (A) In the process of poling, the centrosymmetric arrangement of chromophores changed into non-centrosymmetric arrangement, then the microscopic β values of the chromophores could be summarized into macroscopic NLO activities (d_{33} values) of polymers; (B) SIG means suitable isolation group; IC means the isolation chromophore; "d–π–a" means the azo chromophore and "D–π–A" means the FTC chromophore; the chemical structure and $\mu\beta$ values were quoted from published literature reports and the conjugated structures of the chromophores used in this paper is similar to them; (C) FTC chromophore with a high $\mu\beta$ value was chosen as the main chromophore, while the azo one as the IC moiety. Accordingly, five FTC-containing molecules with an isolation chromophore were designed.

[a] Department of Chemistry, Wuhan University, Wuhan 430072, China. E-mail: lizhen@whu.edu.cn, lichemlab@163.com
[b] Fujian Institute of Research on the Structure of Matter, The Chinese Academy of Sciences, Fuzhou 350002, China

† Electronic supplementary information (ESI) available: Additional figures, tables, and synthetic routes. See DOI: 10.1039/c6tc04282a

dendrimers), hyperbranched polymers, and dendronized hyperbranched polymers, by utilizing the simple azo chromophore as the typical model.[5] Excitedly, the macroscopic NLO effect, characterized as the d_{33} value, could be dramatically enhanced from $\sim$50 pm V^{-1} to as large as 299 pm V^{-1}, coupled with the improved solubility and thermal stability.[6] Some typical molecules are shown in the ESI† (Chart S1). Summarized from the obtained experimental results, the concepts of "Suitable Isolation Group" and "Isolation Chromophore" were proposed (Fig. 1B and 1C),[7] and a new kind of dendritic polymer, "dendronized hyperbranched polymer" (Chart S1, ESI†), has been designed for the first time.[8]

But, in all our previous cases, the $\mu\beta$ value of the used azo chromophore is only 580 $\times$ 10^{-48} esu (Fig. 1B),[1i] inherently acting as the glass ceiling for the further increase of the macroscopic NLO effects of the azo chromophore-containing polymers, no matter how many efforts we attempted on the optimization of the molecular design, according to the concepts mentioned above.[6b,d,10]

Alternatively, to use chromophores with higher $\mu\beta$ values is a good choice to increase the macroscopic NLO effects, coupled with the rational molecular design (Fig. 1C).[11] However, the previously successful molecular design still works. Prompted by all these thoughts, the FTC type chromophore bearing TCF as a strong acceptor was chosen as an example for the test, partially due to its higher $\mu\beta$ value of 18 000 $\times$ 10^{-48} esu, about 31 times that of azo ones.[9] In order to decrease the much stronger electronic interactions among them, azo chromophores bearing "Suitable Isolation Groups" were introduced to the FTC chromophore as "Isolation Chromophores", with the aim of achieving possibly the higher macroscopic NLO performance of the resultant compounds. Accordingly, as shown in Fig. 1C and 2, five FTC-containing molecules have been synthesized with different linkage modes between the two kinds of chromophores, the azo and FTC ones, in which FTC acted as the main chromophore with the azo one in different numbers as the "Isolation Chromophore". Really, as expected, these five FTC-containing molecules demonstrated very good performance with an ultrahigh d_{33} value of 384 pm V^{-1} at the wavelength of 1950 nm achieved for **M1**. Furthermore, the original FTC chromophore was stable at 240 °C, but its derivatives were always not so thermally stable; the thermal stabilities of these five FTC-containing molecules were enhanced to a larger degree, from the general literature reported around 200 °C to 284 °C here, as an excellent side effect of the rational molecular design.[12] Herein, we would like to report their synthesis, structural characterization, photophysical behavior, and NLO properties in detail.

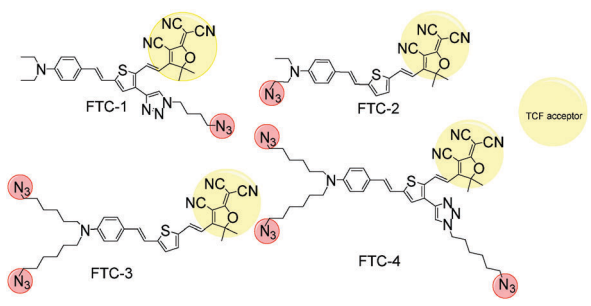

Fig. 2 Chemical structure of four derivatives of FTC.

Results and discussion

Synthesis and characterization

The "click chemistry" reaction was always adopted in our previous work, because many functional groups were tolerant of its mild reaction conditions and the triazole group formed in the reaction was a suitable isolation group.[9,13] So we still used the triazole group as the linker of different chromophore parts and designed four derivatives of FTC containing one or more azido groups, named **FTC-1** to **FTC-4**. As shown in Fig. 2, there is a branch with an azido group attached on the thiophene ring of the FTC part through a triazole group in **FTC-1**. **FTC-2** is used for comparison, which has an azido group at the end of the alkyl chain of the donor. **FTC-3** has two azido groups, in which, there are two azido groups at the end of the two alkyl chains and the alkyl chains are longer than those of **FTC-2**, in order to eliminate the steric hindrance. **FTC-4** has the characteristics of both **FTC-1** and **FTC-3**, which has three azido groups at the end of three long alkyl chains, two at the donor and one at the thiophene ring.

The four derivatives of FTC shared a similar synthetic method, with their synthetic routes being presented in Scheme S1 in the ESI.† Firstly, appropriate aniline vinyl thiophene compounds were synthesized through the Witting–Horner reaction. Then, the bromine atom at the β position of thiophene, if any, was substituted by trimethylsilylacetylene. The hydrogen at the α position of thiophene was substituted by an aldehyde group. Then, the compounds lost a trimethylsilyl group, and the terminal alkyne group reacted with alkyl azide, if there was. Then, all the bromine atoms were substituted by azido groups, which reacted with TCF to yield **FTC-n** as blue powders.

Then, five FTC-containing molecules, **M1** to **M5**, were synthesized through "click chemistry" reactions of **FTC-n** and azo chromophores as shown in Fig. 3, with the proportion of the reactants determined by the proportion of the number of their reactive groups. **M1** to **M4** were prepared from **FTC-n** and compound E. In **M1**, the azo chromophore part was attached to the middle of the FTC part, and its chemical structure is like an "H", which might reduce the dipole–dipole interactions among the chromophore moieties effectively.[14] In comparison with **M1**, **M2** also had one azo chromophore part, but on the donor of the FTC part, and its structure is like a "Z", while **M3** had two azo chromophore parts attached to the donor. **M4** had three azo chromophore parts, with two attached to the donor and one linked to the thiophene ring. **M5** was prepared from **FTC-1** and compound F. Similar to **M1**, **M5** also had an isolation part attached to the middle of the FTC part. However, the difference is that the isolation part has a dendritic structure, which contains three azo chromophore parts.

All the prepared FTC-containing molecules were well characterized, including nuclear magnetic resonance (NMR), infrared

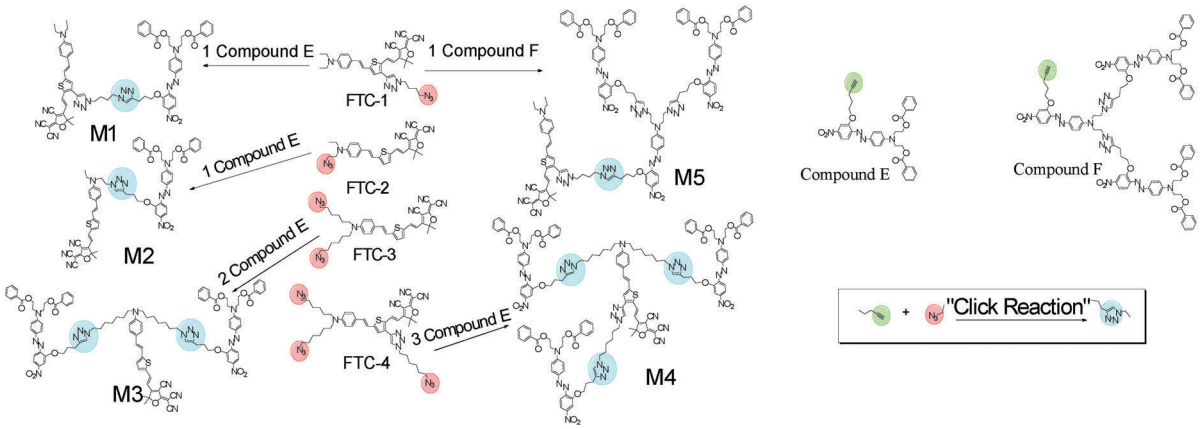

Fig. 3 Synthetic routes of five FTC-containing molecules.

spectroscopy (IR), ultraviolet-visible spectroscopy (UV-vis), thermogravimetric analysis (TGA), differential scanning calorimetry (DSC), elemental analyses (EA), matrix-assisted laser desorption ionization-time of flight-mass spectrometry (MALDI-TOF-MS), with satisfactory data (see the Experimental section and ESI† for detailed analysis data).

Thermal properties

The DSC and TGA curves are shown in Fig. S1 and S2, ESI.† All the prepared molecules of **M1–M5** possess very good thermal stability, with the decomposition temperatures (T_d) (temperatures for 5% weight loss) higher than 250 °C (Table 1). The original FTC was stable at 240 °C, but its derivatives with groups attached to the donor or the thiophene ring through an ester bond always began to decompose at around 200 °C.[12] On the whole, this new type of connection with a triazole group could enhance the thermal stability of FTC derivatives. Their glass transition temperatures (T_g) were in the range of 61–71 °C.

Optical properties

The IR spectra of five FTC-containing molecules are presented in Fig. S3 in the ESI.† Because of the similar chemical bonds in their molecular structures, they have similar IR spectra. In the five IR spectra, there were no peaks at 2140–2100 and 2160–2120 cm^{-1}, indicating the complete reaction of the terminal alkyne groups and azide groups. There was a peak at 1717 cm^{-1}, associated with the –N=N– in the triazole groups. All the five molecules showed absorption bands associated with the nitro groups at about 1518 and 1346 cm^{-1}. They also showed absorption bands at about 2222 cm^{-1}, the typical signal of cyano groups in the TCF acceptor. The UV-vis absorption spectra of **M1** in different solvents are shown in Fig. 4, while those of **M2–M5** are given in Fig. S4 in the ESI,† and their maximum absorption (λ_{max}) wavelengths are summarized in Table 2. There are two absorption peaks in their spectra. The peak at around 460 nm belongs to the azo part, and the other one at about 630 nm should be ascribed to the FTC part. So, to

Table 1 Thermal properties of five compounds

No.	M1	M2	M3	M4	M5
T_g[a] (°C)	65	71	62	61	68
T_d[b] (°C)	277	284	253	271	267
T_e[c] (°C)	117	120	100	92	115
$T_{80\%}$[d] (°C)	102	104	66	70	106

[a] Glass transition temperature. [b] The 5% weight loss temperature. [c] The best poling temperature. [d] The temperature at which d_{33} values decreased to its 80%.

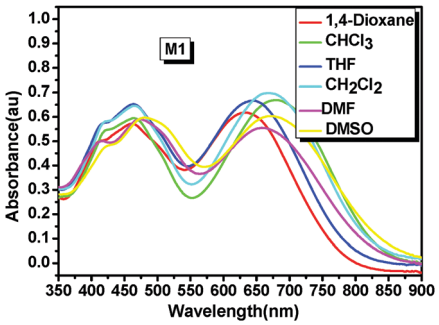

Fig. 4 UV-vis spectra of **M1** in different solvents.

Table 2 The maximum absorption wavelength (λ_{max}, nm) in different solvents (0.02 mg mL^{-1})

Azo part	1,4-Dioxane	$CHCl_3$	THF	CH_2Cl_2	DMF	DMSO	Δ
M1	461	464	464	465	474	480	19
M2	463	459	462	459	492	502	39
M3	461	462	462	463	479	489	28
M4	464	465	465	466	479	487	23
M5	459	459	461	465	474	481	22
FTC part	1,4-Dioxane	$CHCl_3$	THF	CH_2Cl_2	DMF	DMSO	Δ
M1	633	680	644	668	658	671	38
M2	599	631	614	629	626	639	40
M3	623	671	640	664	657	666	43
M4	621	664	635	656	661	666	45
M5	644	683	645	668	661	674	30

$\Delta = \lambda_{max}$ (in DMSO) − λ_{max} (in dioxane); dielectric constant of solvents: 1,4-dioxane = 2.2; $CHCl_3$ = 4.8; THF = 7.5; CH_2Cl_2 = 8.9; DMF = 37.6; DMSO = 46.7.

give a detailed description of the UV-vis absorption spectra of two parts, we analyzed the absorption phenomena in different solvents respectively. For the azo part, the difference of λ_{max} in 1,4-dioxane or DMSO (named Δ value here) of **M1**, was 19 nm, which is the smallest of all. This is reasonable. In the "H" type of combination chromophore **M1**, the shielding effect (to azo part) of the chromophore *via* the isolation chromophore is the strongest of five compounds. A similar phenomenon can also be observed for the FTC part in the spectra, and the Δ value of **M1** is really smaller than others, except that of **M5**. The Δ value for the FTC part in **M5** is 30 nm, which is the smallest one, possibly due to the shielding effect of the bulky dendritic macromolecule attached on the thiophene ring of its FTC part. More effectively shielded chromophores exhibited smaller changes in λ_{max}, since the shielded molecules are less affected by the solvent change.

Spatial geometry

Fig. 5 shows the spatial geometry of the five FTC-containing molecules obtained from the semi-empirical quantum chemistry method. In the structures of **M1** and **M2**, the FTC part trends to the reverse parallel arrangement with the azo part because of the dipole–dipole interaction, and their distances between the two parts are shorter than those of **M3** and **M4** because of the shorter chains between different chromophore parts. In the structure of **M2**, the azo part is near the donor. While in the structure of **M1**, the azo part is near the middle. So the electrostatic screening effect of the azo part in **M1** is better than that of **M2**. In the structure of **M3**, the FTC part also trends to the reverse parallel arrangement with the azo part.

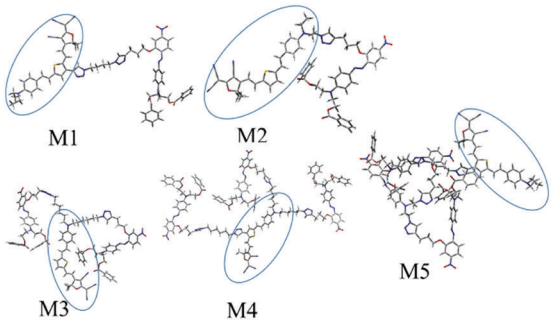

Fig. 5 Optimized chemical structure. FTC parts were in the circles.

Compared to **M1** and **M2**, the arrangement of **M3** has a little chaos. In the structure of **M4**, the azo part is scattered and it surrounded the FTC part. In the structure of **M5**, three azo parts formed a dendritic structure and located on one side of the FTC part. We can make a simple assessment of the electrostatic screening effect of the azo chromophore parts on FTC parts as **M5** > **M1** > **M2**. However, **M4** and **M3** seemed hard to be estimated for the long chains. It coincided with the results of the solvatochromism. Because the dipole–dipole interactions among the FTC part are much stronger than that of the azo part, the electrostatic screening effect on the FTC part from azo parts may be related to their best poling temperatures, during the poling process. The stronger the electrostatic screening effect on the FTC part was, the larger the NLO efficiency related to the FTC part engendered.

NLO properties

To evaluate their NLO activity, the poled thin films of **M1–M5** were fabricated through the convenient spin-coating process. Thanks to their good film-forming properties, high quality thin films were obtained with the thickness in the range of 150 to 350 nm. The most convenient technique to study the second-order NLO activity is to investigate the second harmonic generation (SHG) processes characterized by d_{33}, an SHG coefficient. The method for the calculation of the SHG coefficients (d_{33}) for the poled films has been reported in the literature and our previous papers.

From the experimental data, the d_{33} values of **M1** to **M5** were calculated to be 384, 341, 284, 243 and 326 pm V^{-1}, respectively, at the fundamental wavelength of 1950 nm. To check the reproducibility, we repeated the measurements at least three times and got similar results. Obviously, there is a big difference in the mass fraction of the FTC part in the five FTC-containing molecules. As mentioned in the Introduction part, the $\mu\beta$ value of FTC is much larger than that of the azo chromophore. So the mass fraction of the FTC part may influence the NLO activity. As shown in Table 3, the mass fraction of the FTC part listed from large to small is on the order of **M2** > **M1** > **M3** > **M5** > **M4**. And the d_{33} values of **M1** to **M5** listed from large to small is on the order of **M1** > **M2** > **M5** > **M3** > **M4**. **M1** and **M2** exhibit larger NLO activities, while their mass fraction of FTC is also larger than others. **M4** shows the smallest NLO activity, while its mass fraction of FTC is also

Table 3 Second harmonic generation (SHG) coefficient of FTC-containing molecules and their references

	Mass fraction[a]			(Azo) d_{33}[b] (pm V^{-1})	(FTC) d_{33}[c] (pm V^{-1})	(Azo + FTC) d_{33}[d] (pm V^{-1})	d_{33}[e] (pm V^{-1})
	FTC (%)	G0 (%)	G1 (%)				
M1	37.2	43.0	—	41	223	264	384
M2	41.3	47.7	—	59	193	252	341
M3	24.5	56.6	—	66	231	297	284
M4	17.2	59.5	—	64	137	201	243
M5	19.9	—	69.5	102	213	315	326

[a] Mass fraction of the reference to **M1** to **M5**. G0 and G1 have a similar structure to compound E and compound F without the branch containing the terminal alkyne. [b] The d_{33} values of Azo at 1950 nm. [c] The d_{33} values of the FTC at 1950 nm. [d] The totle d_{33} values of the Azo and FTC at 1950 nm. [e] The d_{33} values of the five compounds at 1950 nm.

the smallest. To deeply investigate the influence of their structure on the NLO effect, another measurement had been carried out for reference. As shown in Table 3, FTC and azo chromophores (G0 and G1) were doped into APC (aliphatic polycarbonate) as the same mass fraction in the corresponding FTC-containing molecules, respectively. Then, 10 kinds of films were made by spin-coating, which were poled at around the T_g of APC with their tested d_{33} values listed in Table 3. The difference between the d_{33} values of **M1** to **M5** and the reference (corresponding (Azo + FTC)) is 120, 89, −13, 42 and 11 pm V^{-1}, respectively.

Compared **M1** with **M2**, the d_{33} value of **M1** is 43 pm V^{-1} larger than that of **M2**, and the mass fraction of FTC part of **M1** (37.2%) is smaller than that of **M2** (47.3%), with the difference of the d_{33} values of **M1** and its reference (120 pm V^{-1}) much larger than that of **M2** (89 pm V^{-1}). Thus, it might be concluded that the connection of the azo chromophore moiety to the middle of FTC should be better for the macroscopic NLO effect, rather than to the donor side, probably due to the good shielding effect, which is partially in accordance with the results observed in their UV-visible spectra. Only **M3** got a smaller d_{33} value than its reference, indicating that the structure with two isolation chromophore moieties attached to the donor side of the main chromophore could not improve the macroscopic NLO activity effectively. Comparing **M5** with **M4**, the d_{33} value of **M5** is 83 pm V^{-1} larger than that of **M4**, since the mass fraction of the FTC part in **M5** (19.9%) is larger than that of **M4** (17.2%). Thus, the larger d_{33} value might not mean that the structure of **M5** is better. Actually, the difference of d_{33} values of **M4** and its reference (42 pm V^{-1}) is larger than that of **M5** (11 pm V^{-1}), so another conclusion might be summarized that the isolation part with a big dendritic structure attached to the middle of FTC is worse than the case scattered and/or surrounded the main chromophore part.

From the experimental results, for FTC-containing molecules, the NLO activity should be mainly dependent on two major factors: the mass fraction of the FTC part and the chemical structure. That is to say, the largest d_{33} value of **M1** is not only due to the high mass fraction of the FTC part, but also due to the good shielding effect between two chromophore parts, which is consistent with the result of solvatochromism.

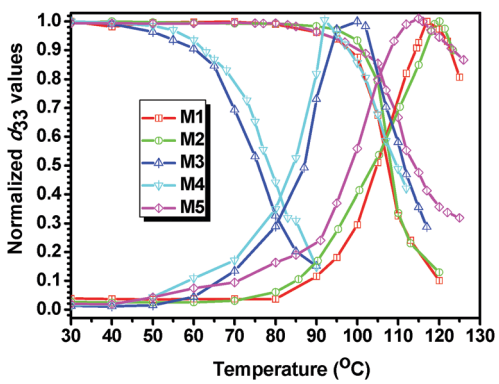

Fig. 6 Poling and decay curves of five compounds.

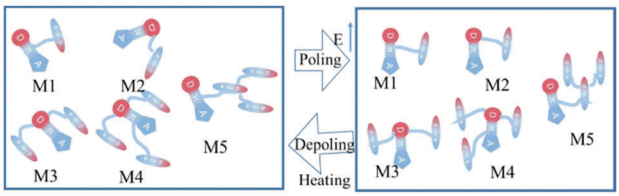

Fig. 7 Graphical illustration of the poling procedure for **M1** to **M5**.

The poling and depoling curves are shown in Fig. 6, while Table 1 summarizes the thermal properties of films in the poling process. The best poling temperatures of **M1** to **M5** are 117, 120, 100, 92 and 115 °C, respectively. In accordance with the analysis of spatial geometry, **M3** and **M4** were more easily poled than others. And because of the bad electrostatic screening effect on the FTC part, **M2** got the highest best poling temperature (120 °C). On the whole, relatively, all the five films are easily poled, with the best poling temperatures far less than their decomposition temperatures (253–284 °C) and about 40–50 °C higher than their glass transition temperatures. Their depoling temperatures (the temperature at which d_{33} values decreased to its 80%) are 102, 104, 66, 70 and 106 °C, respectively. As shown in Fig. 7, in the films after poling, chromophores would trend to relax when the temperature was increased, and the constraint on chromophore moieties was influenced by the length of flexible chains between them. For their long and flexible chain, **M3** and **M4** got lower depoling temperatures than others. From Fig. 6, it could be seen that the decay curves of **M1**, **M2** and **M5** showed good stability of NLO activities with resistance to high temperature. The d_{33} values began to decay at around 80 °C and their $T_{80\%}$ (the temperature at which d_{33} values decreased to its 80%) values were up to 100 °C. In **M5**, three azo chromophore parts formed a dendritic structure, which kept the orientation and limited the freedom of movement. Thus, **M5** got the highest $T_{80\%}$ of 106 °C.

Two molecules with good NLO performance are shown in Fig. 8. **D1** is a dendrimer in our previous work, it contained two kinds of the azo chromophore part, its d_{33} value is 113 pm V^{-1} (@ 1064 nm) and the decomposition temperature is 282 °C.[15] **M1** has the largest d_{33} value 384 pm V^{-1} (@ 1950 nm) in the five FTC-containing molecules. In comparison with dendrimer **D1**, **M1** has a much larger d_{33} value and similar thermal stability.

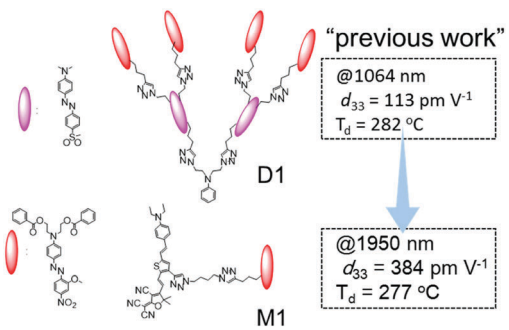

Fig. 8 Comparison between **D1** and **M1**. **D1** was a dendrimer in our previous work.[15]

The good NLO performance is due to the utilization of the chromophore with a high $\mu\beta$ value (the $\mu\beta$ value of FTC is 31 times that of the azo chromophore and the mass fraction of the FTC part of **M1** is 37.2%) and appropriate molecular design (the structure of **M1** is like an ''H''). So this work has achieved the expected results.

Experimental section

Materials and instrumentation

Tetrahydrofuran (THF) was dried over and distilled from K–Na alloy under an atmosphere of dry nitrogen. Dichloromethane and *N*,*N*-dimethylformamide (DMF) were dried over and distilled from CaH_2. Anhydrous ethanol were dried over and distilled from sodium metallic. Compounds A and B, and TCF were synthesized according to the literature method.[12d] Compound E and compound F were synthesized according to our previous work through similar synthetic routes,[5c,13a] and the detailed synthetic procedure is listed in the ESI† (Scheme S1). All other reagents were used as received.

^{1}H and ^{13}C NMR spectra were measured on a Varian Mercury300 spectrometer using tetramethylsilane (TMS; δ = 0 ppm) as an internal standard. The Fourier transform infrared (FTIR) spectra were recorded on a PerkinElmer-2 spectrometer in the region of 3000–500 cm^{-1}. UV-visible spectra were obtained using a Shimadzu UV-2550 spectrometer. Matrix-assisted laser desorption ionization time-of-flight mass spectra were recorded on a Voyager-DE-STR MALDI-TOF mass spectrometer (MALDI-TOF MS; ABI, American) equipped with a 337 nm nitrogen laser and a 1.2 m linear flight path in positive ion mode. Elemental analyses (EA) were performed using a CARLOERBA-1106 microelemental analyzer. Thermogravimetric analysis (TGA) was performed on a NETZSCH STA449C thermal analyzer at a heating rate of 10 °C min^{-1} under nitrogen at a flow rate of 50 cm^3 min^{-1}. The thermal transitions were investigated using a METTLER differential scanning calorimeter DSC822e under nitrogen at a scanning rate of 10 °C min^{-1}. The thickness of the films was measured with an Ambios Technology XP-2 profilometer.

Synthesis

The synthetic routes of four derivatives of FTC (named **FTC-1** to **FTC-4**) are listed in the ESI.† The synthetic routes of five target products are shown as follows.

M1. Under an atmosphere of dry nitrogen, a solution of **FTC-1** (64.4 mg, 0.098 mmol), compound E (61 mg, 0.098 mmol), copper sulfate pentahydrate (2.4 mg, 10% mmol), sodium bicarbonate (1.7 mg, 20% mmol), and sodium L-ascorbate (3.5 mg, 20% mmol) in 3/0.6 mL of THF/H_2O was stirred at 28–30 °C for 3 h. Then the reaction mixture was poured into water and extracted with CH_2Cl_2 three times (50 mL × 3). The combined organic solution was dried over anhydrous sodium sulfate and condensed *via* rotary evaporation. The residue was purified by column spectroscopy on silica gel using the solvents of CH_2Cl_2 and ethyl acetate (2 : 1) as an eluent to give 85 mg of the product (yield 70.0%). ^{1}H NMR (300 MHz, $CDCl_3$, 298 K), δ (TMS, ppm): 8.96–8.91 (d, J = 15.3 Hz, H, –CH═), 8.01–7.99 (m, 4H, ArH), 7.94–7.91 (m, 2H, ArH), 7.87–7.82 (m, 3H, ArH, –CH═), 7.68–7.65 (m, H, ArH), 7.59–7.54 (m, 2H, ArH), 7.45–7.37 (m, 7H, ArH), 7.26 (m, H, ArH), 7.12–6.97 (m, 4H, ArH, –CH═), 6.66 (m, 3H, –CH═, ArH), 4.58–4.56 (m, 4H, $-CH_2-$), 4.41 (m, 2H, $-CH_2-$), 4.34 (m, 2H, $-CH_2-$), 4.28–4.26 (m, 2H, $-CH_2-$), 3.95 (m, 4H, $-CH_2-$), 3.41 (m, 4H, $-CH_2-$), 3.02–2.98 (m, 2H, $-CH_2-$), 2.35–2.31 (m, 2H, $-CH_2-$), 1.96 (m, 4H, $-CH_2-$), 1.78 (s, 6H, $-CH_3$), 1.22 (m, 6H, $-CH_3$). ^{13}C NMR (75 MHz, $CDCl_3$, 298 K), δ (ppm): 175.87, 173.98, 166.39, 155.11, 152.96, 150.79, 148.76, 148.23, 147.00, 146.82, 144.90, 142.63, 140.02, 135.52 133.22, 132.16, 129.53, 129.15, 128.42, 126.12, 125.79, 122.56, 122.47, 121.37, 117.36, 116.38, 114.72, 112.40, 111.87, 111.73, 111.52, 109.22, 97.40, 68.74, 61.63, 49.82, 49.55, 49.04, 44.42, 28.34, 26.94, 26.84, 26.44, 21.84, 12.57. $C_{69}H_{66}N_{14}O_8S$ (EA) (%, found/calcd): C, 66.13/66.22; H, 5.35/5.32; N, 15.83/15.67; S, 2.77/2.56. HR-ESI-MS: m/z for $C_{69}H_{66}N_{14}O_8S$ (found/calcd): $[M + H]^+$: 1251.4984/1251.4982.

M2. Similar to the preparation of **M1**, **M2** was synthesized from **FTC-2** and compound E as a dark powder (63 mg, 64.7%). ^{1}H NMR (300 MHz, $CDCl_3$, 298 K), δ (TMS, ppm): 8.01–7.99 (m, 4H, ArH), 7.93–7.86 (m, 4H, ArH), 7.79–7.74 (m, 2H, ArH, –CH═), 7.68–7.65 (m, H, ArH), 7.59–7.54 (m, 2H, ArH), 7.45–7.40 (m, 5H, ArH, –CH═), 7.34–7.29 (m, 3H, ArH), 7.21 (1, H, –CH═), 7.04–6.95 (m, 3H, ArH, –CH═), 6.58–6.49 (m, 3H, –CH═, ArH), 4.59–4.55 (m, 4H, $-CH_2-$), 4.48–4.46 (m, 2H, $-CH_2-$), 4.12–4.08 (m, 2H, $-CH_2-$), 3.96–3.92 (m, 4H, $-CH_2-$), 3.80 (m, 2H, $-CH_2-$), 3.22–3.20 (m, 2H, $-CH_2-$), 2.99–2.95 (m, 2H, $-CH_2-$), 2.26–2.22 (m, 2H, $-CH_2-$), 1.75 (s, 6H, $-CH_3$), 1.08–1.03 (t, J = 7.5 Hz, 3H, $-CH_3$). ^{13}C NMR (75 MHz, $CDCl_3$, 298 K), δ (ppm): 172.91, 166.39, 155.08, 153.74, 150.75, 148.26, 147.80, 146.87, 146.81, 144.93, 139.27, 137.51, 137.40, 134.03, 133.24, 129.52, 129.46, 128.89, 128.52, 128.47, 127.10, 126.12,124.25, 122.35, 117.41, 116.40, 112.14, 111.84, 111.43, 110.93, 109.26, 96.98, 68.61, 61.60, 50.24, 49.81, 47.96, 45.14, 28.43, 26.39, 21.67, 11.95. $C_{63}H_{57}N_{11}O_8S$ (EA) (%, found/calcd): C, 66.99/67.07; H, 5.10/5.09; N, 13.64/13.66; S, 2.97/2.84. HR-ESI-MS: m/z for $C_{63}H_{57}N_{11}O_8S$ (found/calcd): $[M + H]^+$: 1128.4191/1128.4185.

M3. Similar to the preparation of **M1**, **M3** was synthesized from **FTC-3** and compound E as a dark powder (54 mg, 75.5%). ^{1}H NMR (300 MHz, $CDCl_3$, 298 K), δ (TMS, ppm): 8.02–7.99 (m, 8H, ArH), 7.94–7.87 (m, 8H, ArH), 7.79–7.74 (m, 3H, ArH, –CH═), 7.68–7.65 (m, 2H, ArH), 7.59–7.54 (m, 4H, ArH), 7.45–7.40 (m, 8H, ArH, –CH═), 7.33–7.26 (m, 3H, ArH, –CH═), 7.04–6.95 (m, 7H, ArH, –CH═), 6.56–6.53 (m, 3H, –CH═, ArH), 4.57 (m, 8H, $-CH_2-$), 4.27–4.25 (m, 8H, $-CH_2-$), 3.95 (m, 8H, $-CH_2-$), 3.23(m, 4H, $-CH_2-$), 3.02–2.98 (m, 4H, $-CH_2-$), 2.33–2.31 (m, 4H, $-CH_2-$), 1.84 (m, 2H, $-CH_2-$), 1.74 (s, 6H, $-CH_3$), 1.59 (m, 4H, $-CH_2-$), 1.30 (m, 10H, $-CH_2-$). ^{13}C NMR (75 MHz, $CDCl_3$, 298 K), δ (ppm): 174.27, 166.36, 155.12, 150.79, 148.21, 146.87, 146.70, 144.91, 142.64, 139.64, 133.20, 129.51, 128.40, 126.11, 122.66, 121.14, 121.02, 117.37, 116.36, 111.87, 109.24, 68.79, 68.70, 61.63, 50.08, 49.79, 49.66, 29.76, 29.69, 28.42, 26.50, 26.27, 25.54, 21.86. $C_{106}H_{104}N_{18}O_{15}S$ (EA) (%, found/calcd): C, 66.94/66.93; H, 5.49/5.51; N, 13.30/13.25;

S, 1.70/1.69. MS (MALDI-TOF): *m*/*z* for $C_{106}H_{104}N_{18}O_{15}S$ (found/calcd): $[M + Na]^+$: 1924.6/1923.7.

M4. Similar to the preparation of **M1**, **M4** was synthesized from **FTC-4** and compound E as a dark powder (65 mg, 50.3%). ^{1}H NMR (300 MHz, $CDCl_3$, 298 K), δ (TMS, ppm): 9.02–8.96 (d, J = 15.9 Hz, H, –CH═), 8.01–7.99 (m, 12H, ArH), 7.94–7.91 (m, 12H, ArH), 7.83 (m, 3H, ArH, –CH═), 7.67–7.64 (m, 3H, ArH), 7.56–7.53 (m, 6H, ArH), 7.44–7.40 (m, 12H, ArH), 7.33–7.30 (m, 3H, ArH), 7.03–6.95 (m, 8H, ArH, –CH═), 6.64–6.53 (m, 3H, –CH═, ArH), 4.57 (m, 12H, $-CH_2-$), 4.37 (m, 2H, $-CH_2-$), 4.27–4.25 (m, 12H, $-CH_2-$), 4.15–4.11 (m, 4H, $-CH_2-$), 3.94 (m, 14H, $-CH_2-$), 3.23 (m, 4H, $-CH_2-$), 3.00 (m, 6H, $-CH_2-$), 2.33 (m, 6H, $-CH_2-$), 2.05 (m, 4H, $-CH_2-$), 1.80 (m, 8H, $-CH_2-$, $-CH_3$), 1.51 (m, 4H, $-CH_2-$), 1.28–1.26 (m, 8H, $-CH_2-$). ^{13}C NMR (75 MHz, $CDCl_3$, 298 K), δ (ppm): 175.95, 172.83, 166.37, 155.12, 150.76, 148.28, 146.91, 146.70, 144.96, 139.08, 137.77, 137.28, 134.34, 133.21, 129.08, 129.78, 129.52, 128.93, 128.41, 126.84, 126.11, 123.09, 120.95, 117.42, 116.39, 115.58, 111.86, 111.65, 111.48, 109.24, 96.82, 68.75, 61.63, 50.68, 49.87, 49.79, 30.09, 29.66, 29.58, 29.49, 29.41, 29.20, 29.13, 28.41, 27.10, 26.98, 26.39, 26.30, 26.24, 21.86. $C_{149}H_{148}N_{28}O_{22}S$ (EA) (%, found/calcd): C, 65.94/65.92; H, 5.50/5.49; N, 14.46/14.45; S, 1.19/1.18. MS (MALDI-TOF): *m*/*z* for $C_{149}H_{148}N_{28}O_{22}S$ (found/calcd): $[M + Na]^+$: 2737.3/2736.0.

M5. Similar to the preparation of **M1**, **M5** was synthesized from **FTC-1** and compound F as a dark powder (74 mg, 56.0%). ^{1}H NMR (300 MHz, $CDCl_3$, 298 K), δ (TMS, ppm): 8.90–8.85 (d, J = 15.6 Hz, H, –CH═), 8.00–7.97 (m, 8H, ArH), 7.88–7.71 (m, 14H, ArH, –CH═), 7.61–7.52 (m, 7H, ArH), 7.44–7.27 (m, 11H, ArH), 7.15 (s, 2H, –CH═), 7.06–6.88 (m, 6H, ArH, –CH═), 6.64–6.62 (m, 2H, ArH), 6.53–6.52 (m, 2H, ArH), 6.47–6.41 (d, J = 15.6 Hz, H, –CH═), 4.55 (m, 6H, $-CH_2-$), 4.39 (m, 8H, $-CH_2-$), 4.19 (m, 2H, $-CH_2-$), 4.09 (m, 4H, $-CH_2-$), 3.93 (m, 8H, $-CH_2-$), 3.74 (m, 4H, $-CH_2-$), 3.40–3.38 (m, 4H, $-CH_2-$), 2.93 (m, 6H, $-CH_2-$), 2.21 (m, 6H, $-CH_2-$), 1.96 (m, 6H, $-CH_2-$, $-CH_3$), 1.74 (m, 6H, $-CH_2-$), 1.25–1.16 (m, 6H, $-CH_3$). ^{13}C NMR (75 MHz, $CDCl_3$, 298 K), δ (ppm): 176.12, 173.96, 166.35, 155.31, 155.02, 153.15, 150.75, 149.16, 148.99, 148.12, 147.04, 146.70, 144.80, 142.16, 140.00, 139.00, 133.20, 132.34, 129.50, 129.44, 129.14, 128.40, 126.09, 125.94, 122.45, 122.39, 117.28, 116.34, 111.91, 111.81, 111.57, 111.48, 109.15, 97.42, 68.46, 61.60, 51.10, 49.79, 47.44, 44.40, 29.29, 29.20, 28.31, 26.96, 26.35, 21.69, 12.55. $C_{125}H_{120}N_{28}O_{18}S$ (EA) (%, found/calcd): C, 64.38/64.31; H, 5.17/5.18; N, 16.81/16.80; S, 1.35/1.37. MS (MALDI-TOF): *m*/*z* for $C_{125}H_{120}N_{28}O_{18}S$ (found/calcd): $[M + Na]^+$: 2356.9/2355.8.

Preparation of thin films

The FTC-containing molecules were dissolved in DCM (concentration, 4 wt%) and the solutions were filtered through syringe filters. Then thin films were spin-coated onto indium-tin-oxide (ITO)-coated glass substrates, which were cleaned by *N*,*N*-dimethylformamide, acetone, distilled water, and THF sequentially in an ultrasonic bath before use. Residual solvent was removed by heating the films in a vacuum oven at 40 °C for 12 hours.

NLO measurement of poled films

The second-order nonlinear optical (NLO) efficiencies of the compounds were measured by an *in situ* second harmonic generation (SHG) experiment using a closed temperature controlled oven with optical windows and three needle electrodes. The films were kept at 45° to the incident beam and poled inside the oven and the conducting planes faced to the laser. Then the laser was lighted and the SHG intensity was monitored simultaneously. The poling temperatures of the five kinds of films were different. They shared the same other poling conditions: voltage, 7.0 kV at the needle point; gap distance, 0.8 cm. The NLO efficiencies were investigated using 1950 nm laser radiation. The doubled frequency signals (975 nm) were detected using an Andor's DU420A-BR-DD CCD after the mixed signals passed through the monochromator and a Y-cut quartz crystal served as the reference.

Conclusions

In this work, we have designed and synthesized a series of second-order nonlinear optical (NLO) molecules containing the FTC chromophore and nitro-based azo moieties (**M1–M5**), stimultaneously, which were synthesized through ''click chemistry'' reactions between four derivatives of the FTC, named **FTC-1** to **FTC-4**, and azo chromophores. **M1–M5** exhibited good thermal stabilities, with decomposition temperatures higher than 250 °C. Excitedly, they possess large NLO activities, with the highest d_{33} value of 384 pm V^{-1} achieved in **M1** at 1950 nm, once again confirming the concepts of ''suitable isolation group'' and ''isolation chromophore'' and the advantages of the ''H''-shaped structure. The successful application of these concepts to FTC-based materials with higher $\mu\beta$ values might open up a new avenue for the further development of organic NLO materials to pursue better performance.

Acknowledgements

This work was supported by the National Natural Science Foundation of China (No. 21325416).

Notes and references

1 (*a*) D. M. Burland, R. D. Miller and C. A. Walsh, *Chem. Rev.*, 1994, **94**, 31–75; (*b*) T. J. Marks and M. A. Ratner, *Angew. Chem., Int. Ed. Engl.*, 1995, **34**, 155–173; (*c*) D. Yu, A. Gharavi and L. Yu, *J. Am. Chem. Soc.*, 1995, **117**, 11680–11686; (*d*) S. R. Marder, B. Kippelen, A. K. Y. Jen and N. Peyghambarian, *Nature*, 1997, **388**, 845–851; (*e*) Y. Shi, C. Zhang, H. Zhang, J. H. Bechtel, L. R. Dalton, B. H. Robinson and W. H. Steier, *Science*, 2000, **288**, 119–122; (*f*) M. Lee, H. E. Katz, C. Erben, D. M. Gill, P. Gopalan, J. D. Heber and D. J. McGee, *Science*, 2002, **298**, 1401–1403; (*g*) Y. Bai, N. Song, J. P. Gao, X. Sun, X. Wang, G. Yu and Z. Wang, *J. Am. Chem. Soc.*, 2005, **127**, 2060–2061; (*h*) C. V. McLaughlin, L. M. Hayden, B. Polishak, S. Huang, J. Luo, T.-D. Kim and A. K.-Y. Jen, *Appl. Phys. Lett.*,

2008, **92**, 151107; (*i*) J. Luo, X.-H. Zhou and A. K. Y. Jen, *J. Mater. Chem.*, 2009, **19**, 7410–7424; (*j*) L. R. Dalton, P. A. Sullivan and D. H. Bale, *Chem. Rev.*, 2010, **110**, 25–55; (*k*) J. Luo, S. Huang, Z. Shi, B. M. Polishak, X.-H. Zhou and A. K. Y. Jen, *Chem. Mater.*, 2011, **23**, 544–553.

2 (*a*) B. H. Robinson and L. R. Dalton, *J. Phys. Chem. A*, 2000, **104**, 4785–4795; (*b*) B. H. Robinson, L. R. Dalton, A. W. Harper, A. Ren, F. Wang, C. Zhang, G. Todorova, M. Lee, R. Aniszfeld, S. Garner, A. Chen, W. H. Steier, S. Houbrecht, A. Persoons, I. Ledoux, J. Zyss and A. K. Y. Jen, *Chem. Phys.*, 1999, **245**, 35–50; (*c*) L. R. Dalton, W. H. Steier, B. H. Robinson, C. Zhang, A. Ren, S. Garner, A. Chen, T. Londergan, L. Irwin, B. Carlson, L. Fifield, G. Phelan, C. Kincaid, J. Amend and A. Jen, *J. Mater. Chem.*, 1999, **9**, 1905–1920.

3 (*a*) Z. Li, Q. Li and J. Qin, *Poly. Chem.*, 2011, **2**, 2723; (*b*) W. Wu, R. Tang, Q. Li and Z. Li, *Chem. Soc. Rev.*, 2015, **44**, 3997–4022; (*c*) Z. Li, *Sci. China: Chem.*, 2015, **58**, 969; (*d*) G. Liu, P. Chen, R. Tang and Z. Li, *Sci. China: Chem.*, DOI: 10.1007/s11426-016-0250-5; (*e*) W. Wu, R. Xiao, W. Xiang, Z. Wang and Z. Li, *J. Phys. Chem. C*, 2015, **119**, 14281–14287.

4 (*a*) T. D. Kim, J. W. Kang, J. Luo, S. H. Jang, J. W. Ka, N. Tucker, J. B. Benedict, L. R. Dalton, T. Gray, R. M. Overney, D. H. Park, W. N. Herman and A. K. Jen, *J. Am. Chem. Soc.*, 2007, **129**, 488–489; (*b*) M. Ronchi, A. O. Biroli, D. Marinotto, M. Pizzotti, M. C. Ubaldi and S. M. Pietralunga, *J. Phys. Chem. C*, 2011, **115**, 4240–4246; (*c*) D. B. Knorr, Jr., S. J. Benight, B. Krajina, C. Zhang, L. R. Dalton and R. M. Overney, *J. Phys. Chem. B*, 2012, **116**, 13793–13805.

5 (*a*) Z. Li, Z. Li, C. Di, Z. Zhu, Q. Li, Q. Zeng, K. Zhang, Y. Liu, C. Ye and J. Qin, *Macromolecules*, 2006, **39**, 6951–6961; (*b*) W. Wu, Y. Fu, C. Wang, C. Ye, J. Qin and Z. Li, *Chem. – Asian J.*, 2011, **6**, 2787–2795; (*c*) R. Tang and Z. Li, *Chem. Rec.*, 2016, DOI: 10.1002/tcr.201600065.

6 (*a*) Z. Li, G. Yu, Y. Liu, C. Ye, J. Qin and Z. Li, *Macromolecules*, 2009, **42**, 6463–6472; (*b*) R. Tang, S. Zhou, Z. Cheng, G. Yu, Q. Peng, H. Zeng, G. Guo, Q. Li and Z. Li, *Chem. Sci.*, 2016, DOI: 10.1039/C6SC02956F; (*c*) R. Tang, H. Chen, S. Zhou, B. Liu, D. Gao, H. Zeng and Z. Li, *Polym. Chem.*, 2015, **6**, 6680–6688; (*d*) R. Tang, S. Zhou, W. Xiang, Y. Xie, H. Chen, Q. Peng, G. Yu, B. Liu, H. Zeng, Q. Li and Z. Li, *J. Mater. Chem. C*, 2015, **3**, 4545–4552.

7 W. Wu, C. Li, G. Yu, Y. Liu, C. Ye, J. Qin and Z. Li, *Chem.–Eur. J.*, 2012, **18**, 11019–11028.

8 W. Wu, L. Huang, Y. Fu, C. Ye, J. Qin and Z. Li, *Chin. Sci. Bull.*, 2013, **58**, 2753–2761.

9 L. R. Dalton, *OPTICE*, 2000, **39**, 589–595.

10 (*a*) W. Wu, C. Ye, J. Qin and Z. Li, *ACS Appl. Mater. Interfaces*, 2013, **5**, 7033–7041; (*b*) Z. Li, W. Wu, Q. Li, G. Yu, L. Xiao, Y. Liu, C. Ye, J. Qin and Z. Li, *Angew. Chem., Int. Ed.*, 2010, **49**, 2763–2767.

11 (*a*) L. R. Dalton, P. A. Sullivan and D. H. Bale, *Chem. Rev.*, 2010, **110**, 25–55; (*b*) J. D. Luo and A. K. Y. Jen, *IEEE J. Sel. Top. Quantum Electron.*, 2013, **19**, 42–53; (*c*) T.-D. Kim, J. Luo, Y.-J. Cheng, Z. Shi, S. Hau, S.-H. Jang, X.-H. Zhou, Y. Tian, B. Polishak, S. Huang, H. Ma, L. R. Dalton and A. K. Y. Jen, *J. Phys. Chem. C*, 2008, **112**, 8091–8098.

12 (*a*) Y. Yang, H. Xu, F. Liu, H. Wang, G. Deng, P. Si, H. Huang, S. Bo, J. Liu, L. Qiu, Z. Zhen and X. Liu, *J. Mater. Chem. C*, 2014, **2**, 5124–5132; (*b*) F. Liu, H. Xiao, Y. Yang, H. Wang, H. Zhang, J. Liu, S. Bo, Z. Zhen, X. Liu and L. Qiu, *Dyes Pigm.*, 2016, **130**, 138–147; (*c*) T. D. Kim, J. W. Kang, J. Luo, S. H. Jang, J. W. Ka, N. Tucker, J. B. Benedict, L. R. Dalton, T. Gray, R. M. Overney, D. H. Park, W. N. Herman and A. K. Jen, *J. Am. Chem. Soc.*, 2007, **129**, 488–489; (*d*) C. Zhang, C. Wang, L. R. Dalton, H. Zhang and W. H. Steier, *Macromolecules*, 2000, **34**, 253–261.

13 (*a*) R. Tang, H. Chen, S. Zhou, W. Xiang, X. Tang, B. Liu, Y. Dong, H. Zeng and Z. Li, *Poly. Chem.*, 2015, **6**, 5580–5589; (*b*) Q. Zeng, Z. Li, Z. Li, C. Ye, J. Qin and B. Z. Tang, *Macromolecules*, 2007, **40**, 5634–5637; (*c*) Z. Li, W. Wu, P. Hu, X. Wu, G. Yu, Y. Liu, C. Ye, Z. Li and J. Qin, *Dyes Pigm.*, 2009, **81**, 264–272; (*d*) W. Wu, Y. Fu, C. Wang, Z. Xu, C. Ye, J. Qin and Z. Li, *Chin. J. Polym. Sci.*, 2013, **31**, 1415–1423; (*e*) W. Wu, Q. Huang, G. Qiu, C. Ye, J. Qin and Z. Li, *J. Mater. Chem.*, 2012, **22**, 18486; (*f*) W. Wu, L. Huang, C. Song, G. Yu, C. Ye, Y. Liu, J. Qin, Q. Li and Z. Li, *Chem. Sci.*, 2012, **3**, 1256; (*g*) Z. Li, G. Yu, P. Hu, C. Ye, Y. Liu, J. Qin and Z. Li, *Macromolecules*, 2009, **42**, 1589–1596.

14 Z. Li, W. Wu, G. Yu, Y. Liu, C. Ye, J. Qin and Z. Li, *ACS Appl. Mater. Interfaces*, 2009, **1**, 856–863.

15 W. Wu, Q. Huang, G. Xu, C. Wang, C. Ye, J. Qin and Z. Li, *J. Mater. Chem. C*, 2013, **1**, 3226.